Stress–strain analysis of oriented polyethylene

L. E. Govaert*
Centre for Polymers and Composites, Eindhoven University of Technology, PO Box 513, 5600 MB Eindhoven, The Netherlands

and C. W. M. Bastiaansen
Centre for Polymers and Composites, Eindhoven University of Technology, PO Box 513, 5600 MB Eindhoven, The Netherlands; and DSM Research, Geleen, The Netherlands

and P. J. R. Leblans
Agfa-Gevaert, Antwerp, Belgium
(Received 24 December 1991)

The time-dependent deformation behaviour of a commercial grade of high-performance polyethylene fibres (Dyneema SK66), was studied using static and dynamic mechanical testing. A mathematical model is proposed, where the total deformation of the fibre is regarded as being composed of a stress-linear delayed elastic component and a non-linear plastic flow contribution. The thermo-rheological characteristics of the delayed elastic contribution are obtained using dynamic mechanical thermal analysis. The non-linear plastic flow component is characterized separately using long-term creep experiments. Model predictions of stress relaxation and tensile experiments are in good agreement with the experimental data.

(Keywords: polyethylene; fibres; creep; stress relaxation; dynamic behaviour; modelling)

INTRODUCTION

High-performance polyethylene fibres, with tenacities of 3–4 GPa and moduli of 100–150 GPa, are nowadays commercially produced by solution spinning and subsequent drawing of ultra-high-molecular-weight polyethylene (UHMW-PE) ($M_w > 10^3$ kg mol^{-1})[1–6]. The high work to break and the viscoelastic character of these fibres render them eminently suitable for applications where high impact resistance and vibrational damping is required[7–9]. One of the major drawbacks, however, is the pronounced time dependence of the mechanical properties of these fibres (creep, stress relaxation). In exploring new applications for UHMW-PE fibres, the ability to predict the time-dependent behaviour of the fibres in various loading conditions is of great significance.

The long-term mechanical behaviour of melt-spun/drawn high-density polyethylene (HDPE) fibres has been studied extensively by Wilding and Ward[10–14]. They distinguished two separate contributions to the deformation: (a) a linear viscoelastic recoverable component, further referred to as the delayed elastic component; and (b) a non-linear irrecoverable flow component, further referred to as the plastic flow component[10]. Moreover, they showed[10,11] that the plastic flow contribution to the deformation is consistent with two temperature-activated Eyring dashpots acting in parallel. The linear delayed elastic deformation was incorporated into the model by addition of linear springs in series with the dashpots, which made it possible to predict, to some extent, creep[11] and stress relaxation behaviour[12,15]. However, for accurate description of the deformation behaviour over a wide range of stress and temperature, this model requires several sets of parameters, each covering a limited area[15]. Moreover, since the model only contains two relaxation times, it will inevitably poorly represent the dynamic behaviour of the material (vibrational damping).

In previous work[16] the delayed elastic behaviour of UHMW-PE fibres in creep, stress relaxation and tensile experiments was modelled using the classical theory of linear viscoelasticity[17]. However, as the non-linear plastic flow contribution to the deformation was neglected in this approach, the validity of the model is restricted to small deformations and/or short loading times.

In the present investigation, a mathematical model is presented that incorporates both the linear delayed elastic and the non-linear plastic flow contributions to the deformation. The model is based on the assumption that both components are additive and act independently.

To investigate the validity of the stress–strain relation, a commercial grade of high-performance polyethylene fibre (Dyneema SK66) is fully characterized. The stress and temperature dependences of the plastic flow component are obtained by determining plateau creep rates from long-term creep experiments. The linear delayed elastic component is evaluated using dynamic mechanical experiments.

It should be noted that the quantitative characteristic functions obtained in this study are specifically for the

*To whom correspondence should be addressed

0032-3861/93/030534-07

fibre investigated (SK66) and cannot be applied directly to predict the deformation behaviour of any solution-spun fibre. Similar to melt-spun fibres[10,11,14], the mechanical behaviour of solution-spun ultra-drawn polyethylene is strongly influenced by parameters such as molecular weight, molecular-weight distribution, draw ratio and, additionally, polymer concentration in solution[1,4,18–25].

The present investigation is directed to develop a profound mathematical analogue that is capable of predicting the actual deformation behaviour of oriented polyethylene fibres in any loading condition. As such, it provides a new methodology to analyse the effect of processing parameters and intrinsic polymer characteristics on the general performance of oriented polyethylene fibres. Also, the analysis of the deformation behaviour, as presented here, supplies a profound basis for a better understanding of the molecular processes underlying the deformation of oriented polyethylene[26].

EXPERIMENTAL

All experiments in this study have been performed on solution-spun, ultra-drawn UHMW-PE fibres Dyneema SK66, supplied by DSM-HPF as a multi-filament yarn of 1600 denier. The modulus and strength of the fibres were 85 GPa and 3 GPa respectively.

Dynamic experiments were performed in uniaxial extension in the frequency range from 0.2 to 3 Hz, at temperatures from −20 to 105°C. The equipment used for the experiments was a Polymer Laboratories DMTA MK 2. By splitting the multi-filament yarn, samples were prepared with a cross-sectional area of 0.01 mm^2 and a length of 20 mm. To prevent excessive creep of the fibres during the experiment as a result of the static load applied, a relatively low static stress level of 150 MPa was chosen. Further restriction of creep was achieved by reducing the static load at higher temperatures by means of the reduced force option that is available on the apparatus. All scans were performed at least five times and the results were subsequently averaged, resulting in a relative accuracy of 5% for the dynamic modulus E_d and tan δ.

Stress relaxation, creep and constant-strain-rate experiments up to $10^{-3}\,s^{-1}$ were performed on a Frank 81565 tensile tested equipped with an extensometer and a thermostatically controlled oven. Additional tensile experiments with high strain rates (up to $10\,s^{-1}$) were performed on a Zwick Rel servo-hydraulic tensile tester equipped with a thermostatically controlled oven. In all cases the fibre samples had a length of 255 mm. To improve clamping, the fibre ends were provided with cardboard tabs glued together with an epoxy resin.

The stress relaxation experiments, with loading times not exceeding 150 h, were performed at strains of 0.5–2.5% and temperatures of 30–70°C. Creep experiments, with loading times not exceeding 50 h, were performed in dead-weight loading at loads of 200–1500 MPa and temperatures of 30–90°C. Plateau creep rates were determined from the creep data employing the method suggested by Sherby and Dorn[27]. Additional information on the stress dependence of the plateau creep rate at high temperatures was obtained by determining yield stresses from constant-strain-rate experiments at 70 and 90°C.

To examine the development of irrecoverable deformation during creep, fibre samples were loaded at 500 MPa at a temperature of 70°C. For each sample the loading time was varied, and the irrecoverable deformation was measured using the cardboard end tabs as a reference. To exclude any recoverable contribution to the deformation, each sample was allowed to recover at a temperature of 70°C for a period exceeding 10 times the loading time.

RESULTS

General deformation behaviour

In *Figure 1* the creep compliance $D(t) = \varepsilon(t)/\sigma_0$ of the SK66 fibre is presented as a function of time for various temperatures and stresses. The creep curves at 30°C can be regarded as representative of the general creep behaviour. Two important observations can be made: at short loading times the deformation behaviour is nearly stress-linear; while at long loading times the onset to a steady rate of creep is found (observed as an upswing of the curves in the double logarithmic representation of *Figure 1*), which is strongly stress-dependent.

The deformation behaviour observed may be regarded as being typical for oriented polyethylene, since similar observations were made on moderately oriented, melt-spun HDPE fibres by Wilding and Ward, who suggested a phenomenological model consisting of a linear delayed elastic component and a non-linear plastic flow component[10].

This phenomenological interpretation is clarified in *Figure 2*, where the creep deformation of the SK66 fibre (70°C, 500 MPa) is decomposed into its recoverable and irrecoverable components. The irrecoverable deforma-

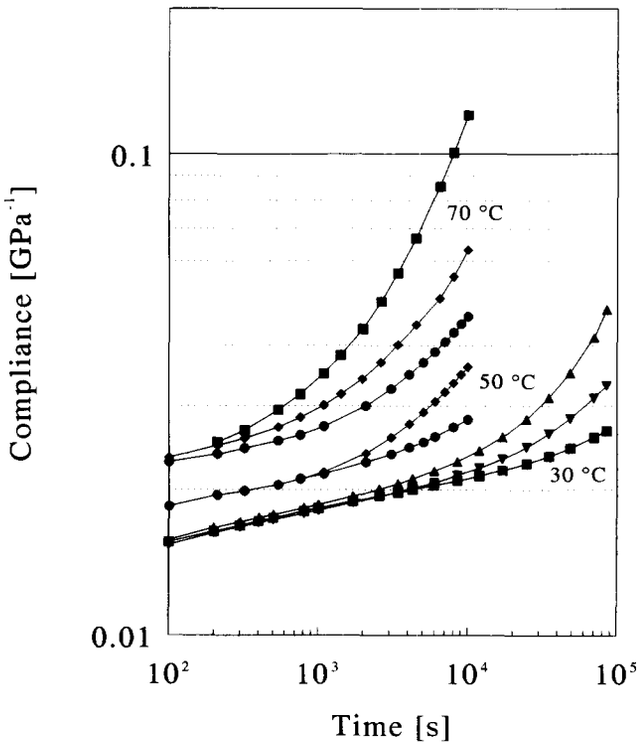

Figure 1 Creep compliance of UHMW-PE yarn (SK66) at various temperature and loads: 250 MPa (●), 400 MPa (◆), 500 MPa (■), 750 MPa (▼) and 1 GPa (▲)

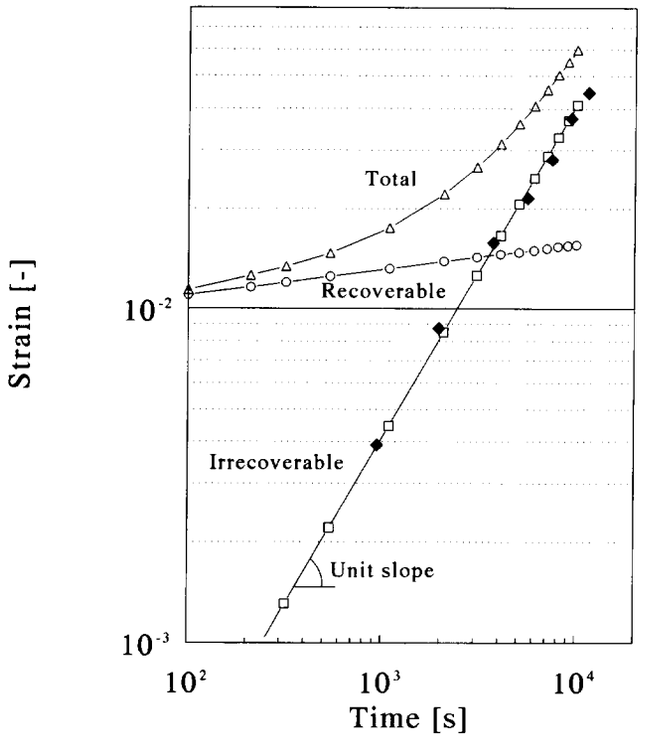

Figure 2 Creep deformation at 70°C and a load of 500 MPa (△), decomposed into its recoverable, delayed elastic (○) and irrecoverable, plastic flow (□) components. Experimental data on irrecoverable deformation are also represented (◆)

tion is observed to increase proportionally with the elapsed loading time or, more specifically, to develop at a constant rate in time. At long loading times this plastic flow component dominates the creep behaviour of the fibres, and a constant rate of creep is found. This constant rate of creep is generally referred to as the plateau creep rate, which, as can be observed in *Figure 1*, is evidently strongly stress- and temperature-dependent.

Since the plastic flow contribution to the creep deformation increases proportionally with the loading time, the delayed elastic component will dominate the deformation behaviour of the fibre at short loading times. Of course, the time region where the stress-linear delayed elastic behaviour dominates (see *Figure 1*) will be determined by the value of the plastic flow rate at a given temperature and stress.

In previous work[16] it was shown that the classical theory of linear viscoelasticity can be applied to the stress-linear (short-time) behaviour of the fibres and can be used to correlate stress relaxation, creep and constant-strain-rate experiments. The applicability of this *linear* viscoelastic stress–strain relation, however, is obviously restricted to a limited time region.

To obtain a unified model that combines the contributions of both the delayed elastic and the plastic components, and, as such, will have a larger range of application, it is assumed that (a) both components act in series with each other, (b) the delayed elastic contribution is not influenced by the plastic flow contribution, and (c) the plastic flow rate is uniquely determined by stress and temperature.

Characterization of the irrecoverable deformation: plateau creep rates

Evidently, long-term creep experiments are pre-eminently suitable to characterize the plastic flow contribution, since at long loading times this component dominates and can be measured directly. At high temperatures, additional information on the stress dependence of the plastic flow contribution can be obtained in deriving yield stresses from constant-strain-rate experiments[14].

The stress dependence of the plateau creep rate, as measured on the SK66 fibres in both creep and constant-strain-rate experiments, is presented for various temperatures in *Figure 3*. Two important observations can be made:

(i) The stress dependence of the plateau creep rate can be represented by a power-law relation in the stress region from 200 to 2000 MPa at all temperatures.

(ii) The power-law slope appears to be independent of temperature.

Apparently, the stress and temperature dependences of the plastic flow rate are independent of each other, which leads to:

$$\dot{\varepsilon}_{pl}(\sigma, T) = a_{pl}(T)C\sigma^{m} \qquad (1)$$

where $C = 4.6 \times 10^{-16}$ MPa^{-m} s^{-1} (reference temperature 70°C) and $m = 3.7$, and the temperature dependence of the plastic flow rate $\dot{\varepsilon}_{pl}$ is represented by the shift factor $a_{pl}(T)$.

This temperature dependence is analysed in *Figure 4*, where the Arrhenius plots of the plastic flow rate at stresses of 200–1000 MPa are constructed. It is evident that the irrecoverable creep can be approximated by a single temperature-activated process with an activation energy of 28 kcal mol^{-1} (118 kJ mol^{-1}) over the entire region of stress and temperature experimentally covered.

Consequently, the temperature shift factor $a_{pl}(T)$ can

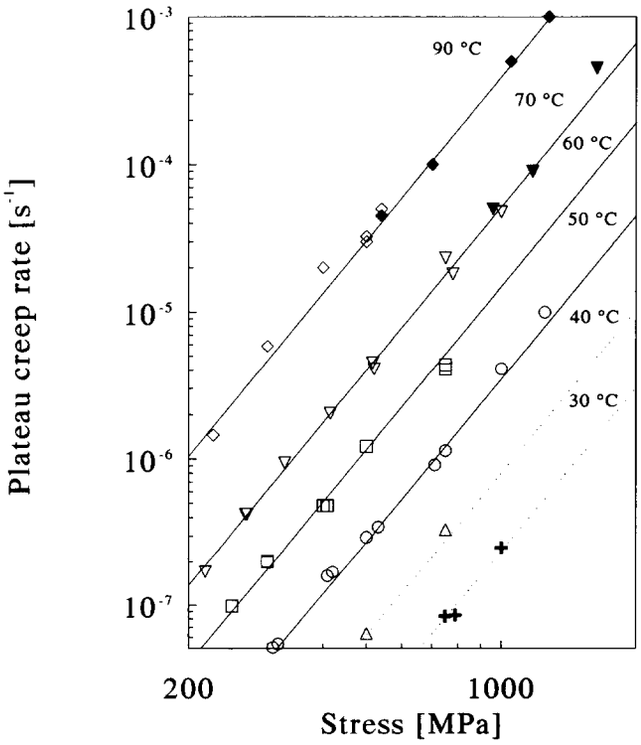

Figure 3 Stress dependence of the plateau creep rate at temperatures of 30°C (+), 40°C (△), 50°C (○), 60°C (□), 70°C (▽) and 90°C (◇). The symbols (▼) and (◆) represent data obtained by constant-strain-rate experiments

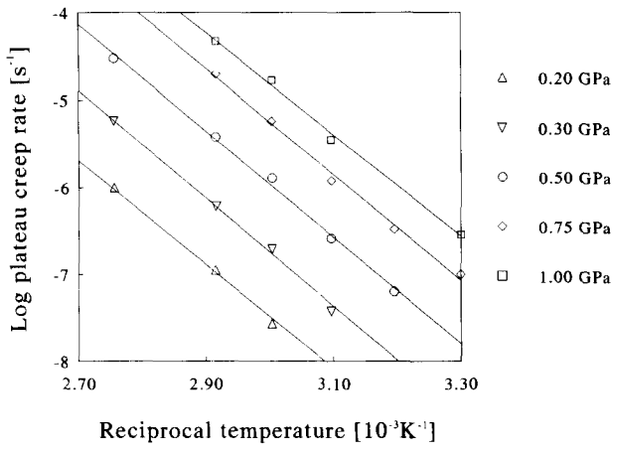

Figure 4 Arrhenius plots of the plateau creep rate at various stresses

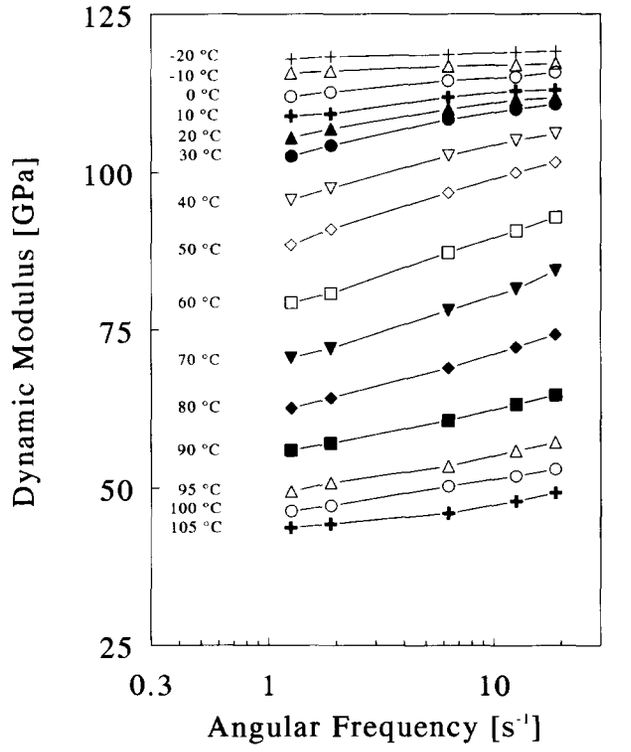

Figure 5 Dynamic modulus of SK66 vs. angular frequency at temperatures from −20 to 105°C

be expressed as:

$$a_{pl}(T) = \exp\left[\frac{U}{R}\left(\frac{1}{T_0} - \frac{1}{T}\right)\right] \qquad (2)$$

where U = Arrhenius activation energy (118 kJ mol^{-1}), R = gas constant (8.314 J mol^{-1} K^{-1}), T = absolute temperature (K) and T_0 = reference temperature (343 K, 70°C).

Although caution should be exercised in using extrapolations far outside the region experimentally covered, the experimental data available justify application of the temperature shift in the temperature range from 30 to 90°C.

Recoverable deformation: thermo-rheological behaviour

An efficient method to isolate the linear viscoelastic contribution experimentally is by dynamic strain excitation at low static stress levels. In these conditions the dynamic stress signal will not be influenced by the irrecoverable deformation process, since, even at high temperatures, the development of irrecoverable strain during a dynamic cycle is negligible. On the other hand, however, the static load applied should not be too high, since excessive irrecoverable deformation (equivalent to post-drawing) leads to an increase of the modulus of the fibres[26].

The experimental data are shown in *Figures 5* and *6*, where the values of the dynamic modulus E_d (*Figure 5*) and tan δ (*Figure 6*) are plotted *versus* the angular frequency for various temperatures. As expected, the dynamic modulus decreases with decreasing frequency at a fixed temperature, as well as with increasing temperature at a fixed frequency. The isotherms of tan δ, on the other hand, increase gradually with decreasing frequency for temperatures up to 70°C, reach their maximum and subsequently decrease with decreasing frequency at higher temperatures. This maximum in tan δ is generally ascribed to the α-relation process[28], and is in accordance with observations of Roy *et al.*[29] and Matsuo *et al.*[30] for solution-cast, ultra-drawn UHMW-PE films, as well as with results of Gibson *et al.* for melt-spun HDPE fibres[31].

Master curves of E_d and tan δ could be constructed by horizontal shifting of adjacent curves. With a relative accuracy of 5%, the same horizontal shift factor superimposes the tan δ curves as well as the dynamic modulus curves. The master curves for E_d and tan δ, at a reference temperature of 30°C, are presented in *Figure 7*. The shift factors $a_{T0}(T)$ used to construct both curves and those derived from stress relaxation experiments are plotted logarithmically against $1/T$ in *Figure 8*.

It is clear that the data in *Figure 8* cannot be represented by a single thermally activated Arrhenius process. The observed temperature dependence of the

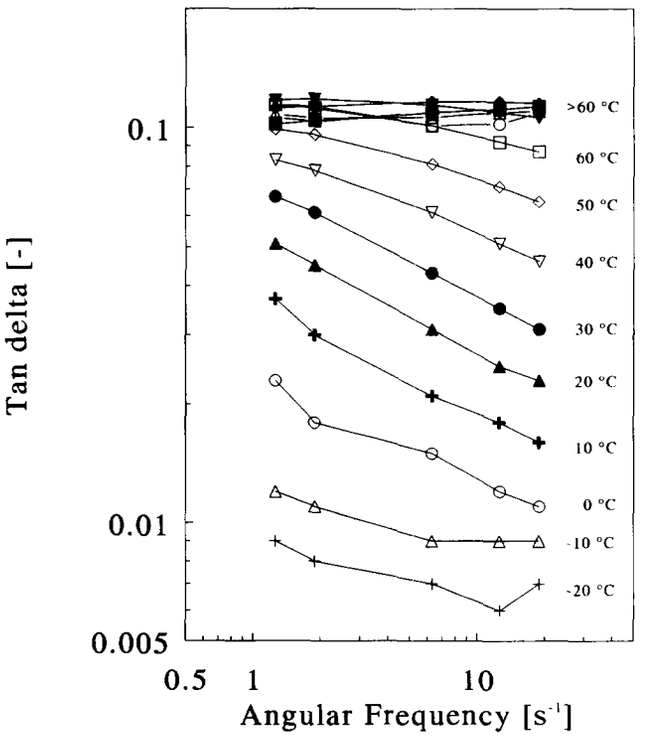

Figure 6 Tan δ of SK66 vs. angular frequency at temperatures from −20 to 105°C

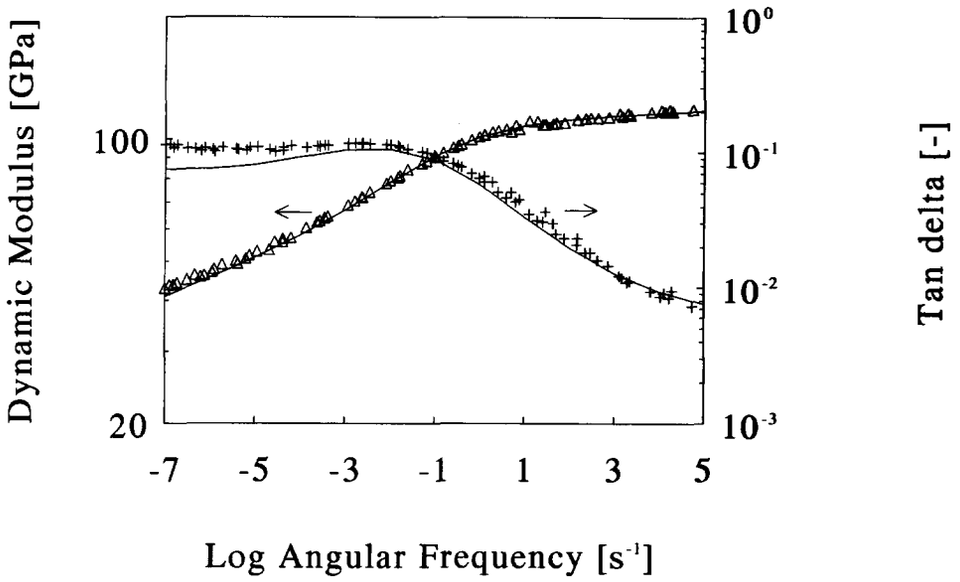

Figure 7 Master curves of the dynamic modulus (△) and tan δ (+) of SK66 vs. the logarithm of the angular frequency for a reference temperature of 30°C. The full curves represent the fit obtained with the continuous relaxation-time spectrum of *Figure 9*

shift factor is generally interpreted in terms of combined contributions of at least two temperature-activated (crystalline) relaxation processes α_1 and α_2, for isotropic[32–34] as well as for oriented polyethylene[29,30]. Of course, the contribution of two separate relaxation processes, possessing different activation energies, would lead to a thermo-rheologically complex behaviour, which implies that short-term experiments at high temperatures cannot easily be translated to long-term behaviour at low temperatures[32].

However, in *Figure 8* a similarity is observed in the temperature dependence of the dynamic data, measured from 0.2 to 5 Hz (short relaxation times), and stress relaxation data, measured from 100 to 10000 s (long relaxation times). This similarity suggests that the material behaviour is thermo-rheologically simple, which is more indicative of a single molecular process. The molecular origin of this deformation process has been studied extensively and is discussed in another paper[26].

With respect to the present investigation, the observed similarity in the temperature dependences of short and long relaxation times indicates that the time–temperature superposition principle does apply over the entire frequency/temperature range. This implies that the constructed master curve (*Figure 7*) can be considered to represent the actual fibre behaviour at 30°C. The shift factors $a_{de}(T)$, presented in *Figure 8*, will be used to translate the fibre behaviour to other temperatures.

In order to obtain a mathematical stress–strain relation for the viscoelastic contribution, the classical theory of linear viscoelasticity is applied[17]. In this theory the stress is related to viscoelastic strain rate by the Boltzmann superposition integral:

$$\sigma(t) = \int_{-\infty}^{t} E(t-t')\dot{\varepsilon}_{de}(t')\,dt' \qquad (3)$$

where σ is the extensional stress, E is the relaxation modulus and $\dot{\varepsilon}_{de}$ is the strain rate acting on the delayed elastic component. It must be emphasized that in our

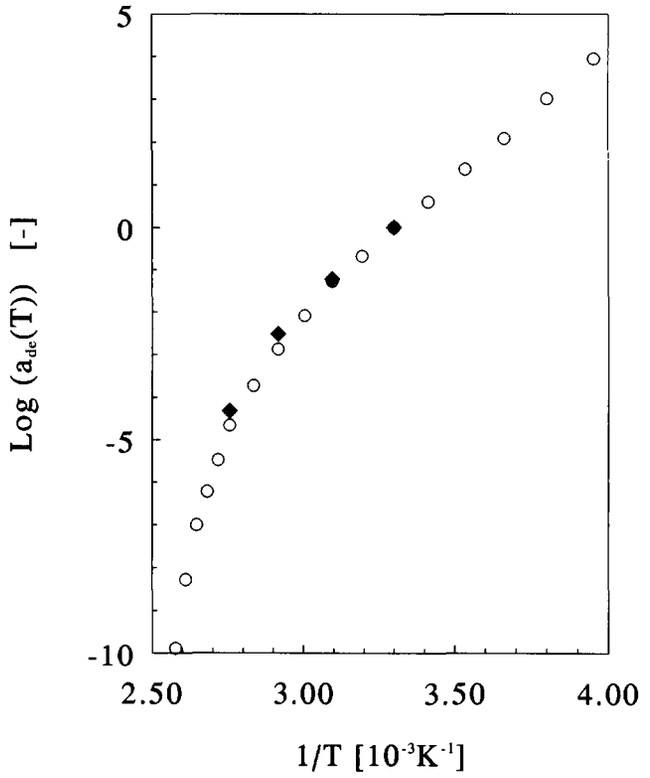

Figure 8 Arrhenius plot of the horizontal shift factor $a_{de}(T)$, for a reference temperature of 30°C: (○) shift factor as derived from the dynamic quantities; (◆) shift factor as derived from stress relaxation experiments in the linear region

case equation (3) is valid for simple extensional deformations only, and cannot be translated directly to other deformation modes.

To specify a stress–strain relation enabling description of the viscoelastic behaviour of UHMW-PE fibres over the entire region covered, a continuous relaxation-time spectrum for the stress relaxation modulus $E(t)$ (ref. 17)

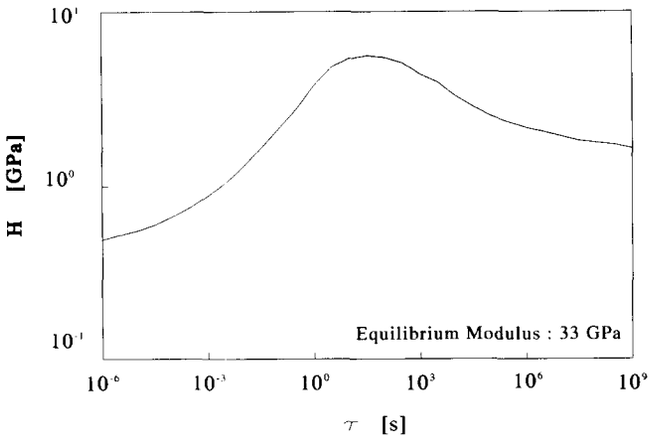

Figure 9 The continuous relaxation-time spectrum $H(\tau)$ of SK66 for a reference temperature of 30°C

is introduced (isothermal conditions):

$$E(t, T) = E_\infty + \int_{-\infty}^{\infty} H(\tau) \exp\left(\frac{-t}{a_{de}(T)\tau}\right) d \ln \tau \quad (4)$$

The lower and upper bounds of the integral are in practice restricted to finite values. An equilibrium modulus E_∞ is introduced to account for the reversible character of the viscoelastic contribution to the deformation.

The procedure used to derive the relaxation-time spectrum $H(\tau)$ is based on an approximate relation, suggested by Booij and Palmen[35], between the relaxation-time spectrum, the dynamic modulus and the loss angle δ. The procedure is described in detail in ref. 36.

Since it proved to be difficult to find a spectrum that gave accurate predictions of both $\tan \delta$ and E_d, the spectrum was constructed primarily for the prediction of the dynamic modulus. The distribution of relaxation times $H(\tau)$ obtained by this procedure is presented in *Figure 9*, whereas a value of 33 GPa was derived for the equilibrium modulus E_∞, which represents the contribution of relaxation times over 10^9 s. The predictions of the master curves of E_d and δ, using the spectrum of *Figure 9*, are presented in *Figure 7*. The spectrum $H(\tau)$ introduced in equations (3) and (4) leads to a stress–strain relation for the delayed elastic component that is applicable over a large frequency/time scale.

Unified modelling

To obtain a unified stress–strain relation that covers the total deformation of UHMW-PE fibres, the delayed elastic and the plastic flow components are regarded to act in series. This leads to the following decomposition of the total strain ε_{tot} of the fibre:

$$\varepsilon_{tot} = \varepsilon_{de} + \varepsilon_{pl} \quad (5)$$

where ε_{de} and ε_{pl} are the contributions to the total strain of the delayed elastic and the plastic flow processes, respectively. The time derivative of equation (5) reads:

$$\dot{\varepsilon}_{de}(\sigma, T) = \dot{\varepsilon}_{tot} - \dot{\varepsilon}_{pl}(\sigma, T) \quad (6)$$

Since the series connection represented by equation (5) implies that the stress responsible for the delayed elastic deformation is the same as the stress responsible for the plastic flow deformation, a stress–total strain relation is obtained by introduction of equation (6) into equation (4), which leads to:

$$\sigma(t, T) = \int_0^t E(t - t', T)[\dot{\varepsilon}_{tot} - \dot{\varepsilon}_{pl}(\sigma, T)] \, dt' \quad (7)$$

where $E(t, T)$ is defined in equation (4) and $\dot{\varepsilon}_{pl}(\sigma, T)$ in equation (1).

Model verification

In order to evaluate the validity of the stress–strain relation, the stress build-up at different constant strain rates and the stress relaxation after different steps in strain were calculated and compared with experimental data. For model predictions, the stress–strain relation, equation (7), was incorporated in a computer program that was specially written for this purpose. The loading time was divided into small time increments, and the deformation rate of the plastic flow contribution was assumed to be constant over an increment. The magnitude of the plastic deformation rate was accordingly recalculated for the next increment. The time steps chosen were sufficiently small to eliminate any influence of the discretization on the calculation results.

Constant-strain-rate experiments were performed at 30 and 70°C, at strain rates of 10^{-4} to $10\,s^{-1}$. *Figure 10* compares the experimental results with numerical predictions, and shows that the model based on series connection of delayed elastic and plastic flow components leads to accurate predictions over the complete range of strain rates.

Model predictions of stress relaxation at various strains are compared with experimental data in *Figure 11*, at temperatures of 30, 50 and 70°C, respectively. At

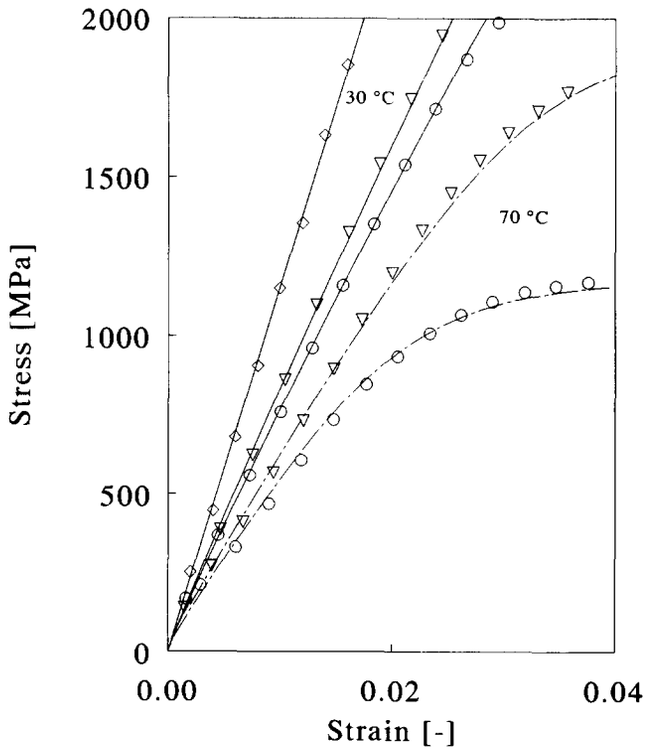

Figure 10 Constant-strain-rate experiments at various temperatures and strain rates of $10^{-4}\,s^{-1}$ (○), $10^{-3}\,s^{-1}$ (▽) and $10\,s^{-1}$ (◇), compared with model predictions (curves)

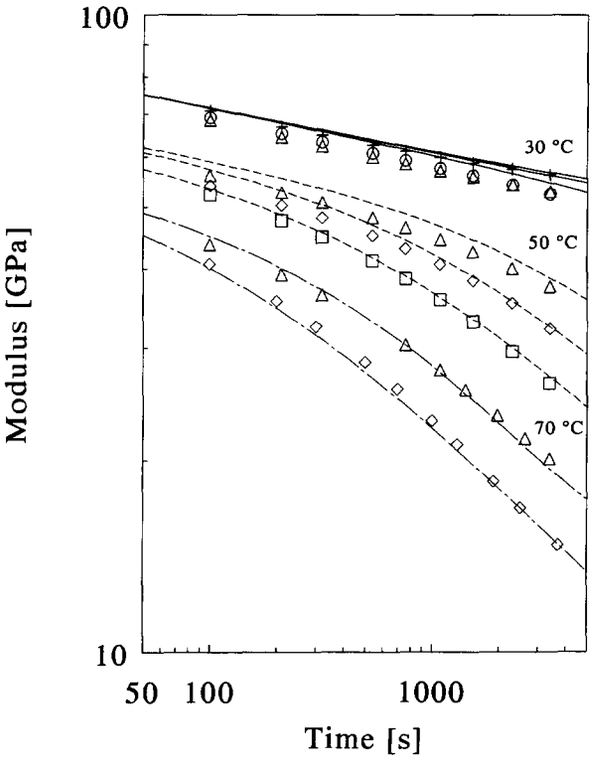

Figure 11 Stress relaxation experiments at various temperatures and strain levels of 0.5% (+), 1.0% (○), 1.5% (△), 2% (◇) and 2.5% (□), in comparison with model predictions (curves)

low strains, where the viscoelastic contribution is dominant, the predicted modulus is higher than experimentally observed, the deviation being within 10%. This inaccuracy indicates that the delayed elastic component is also intrinsically non-linear. At a higher strain, where the plastic flow contribution becomes dominant, the accuracy of the predictions increases significantly.

CONCLUSIONS

A unified model for the combined contribution of the delayed elastic and plastic flow components was obtained by considering the two processes to act in series. Evaluation of the model in stress relaxation and constant-strain-rate experiments (up to impact rate) shows that the deviations between calculated and measured stresses are within 10%. Therefore, it can be concluded that the proposed model gives an accurate representation of the actual deformation behaviour of oriented polyethylene fibres.

REFERENCES

1 Smith, P., Lemstra, P. J., Kalb, B. and Pennings, A. J. *Polym. Bull.* 1979, **1**, 633
2 Smith, P. and Lemstra, P. J. *Makromol. Chem.* 1979, **180**, 2983
3 Smith, P. and Lemstra, P. J. *J. Mater. Sci.* 1980, **15**, 505
4 Smith, P. and Lemstra, P. J. *Colloid. Polym. Sci.* 1980, **258**, 891
5 Lemstra, P. J., van Aerle, N. A. J. M. and Bastiaansen, C. W. M. *Polym. J.* 1987, **19**, 85
6 Lemstra, P. J., Kirschbaum, R., Ohta, T. and Yasuda, H. in 'Developments in Oroented Polymers–2' (Ed. I. M. Ward), Elsevier, London, 1987, p. 39
7 Peijs, A. A. J. M., Catsman, P., Govaert, L. E. and Lemstra, P. J. *Composites* 1990, **21**, 513
8 Peijs, A. A. J. M., Venderbosch, R. W. and Lemstra, P. J. *Composites* 1990, **21**, 522
9 Govaert, L. E., d'Hooghe, E. L. J. C. J. and Peijs, A. A. J. M. *Composites* 1991, **22**, 113
10 Wilding, M. A. and Ward, I. M. *Polymer* 1978, **19**, 969
11 Wilding, M. A. and Ward, I. M. *Polymer* 1981, **22**, 870
12 Wilding, M. A. and Ward, I. M. *J. Mater. Sci.* 1984, **19**, 629
13 Wilding, M. A. and Ward, I. M. *Plast. Rubber Proc. Appl.* 1981, **1**, 167
14 Wilding, M. A. and Ward, I. M. *J. Polym. Sci., Polym. Phys. Edn* 1984, **22**, 561
15 Sweeney, J. and Ward, I. M. *J. Mater. Sci.* 1990, **25**, 697
16 Leblans, P. J. R., Bastiaansen, C. W. M. and Govaert, L. E. *J. Polym. Sci., Polym. Phys. Edn* 1989, **27**, 1009
17 Ferry, J. D. 'Viscoelastic Properties of Polymers', Wiley, New York, 1980
18 Ward, I. M. *Polym. Eng. Sci.* 1984, **24**, 724
19 Smith, P. and Lemstra, P. J. *Polymer* 1980, **21**, 1341
20 Smith, P., Lemstra, P. J. and Booij, H. C. *J. Polym. Sci., Polym. Phys. Edn* 1981, **19**, 877
21 Smith, P. and Lemstra, P. J. *J. Polym. Sci., Polym. Phys. Edn* 1980, **19**, 1007
22 Smith, P. and Lemstra, P. J. *J. Polym. Sci., Polym. Phys. Edn* 1982, **20**, 2229
23 Bastiaansen, C. W. M. PhD Thesis, Eindhoven University of Technology, 1991
24 Bastiaansen, C. W. M. *Polymer* 1992, **33**, 1649
25 Bastiaansen, C. W. M. and Grooters, G. P. *Polymer* 1992, **33**, 1653
26 Govaert, L. E. and Lemstra, P. J. *Colloid. Polym. Sci.* 1992, **270**, 455 Govaert, L. E. PhD Thesis, Eindhoven University of Technology, 1990
27 Sherby, O. D. and Dorn, J. E. *J. Mech. Phys. Solids* 1958, **6**, 145
28 Boyd, R. H. *Polymer* 1985, **26**, 323
29 Roy, S. K., Kyu, T. and St John Manley, R. *Macromolecules* 1988, **21**, 1741
30 Matsuo, M., Sawatari, C. and Ohhata, T. *Macromolecules* 1988, **21**, 1317
31 Gibson, A. G., Davies, G. R. and Ward, I. M. *Polymer* 1978, **19**, 683
32 Nakayasu, H., Markovitz, H. and Plazek, D. J. *Trans. Soc. Rheol.* 1961, **5**, 261
33 Ribes Greus, A. and Diaz Calleja, R. J. *J. Appl. Polym. Sci.* 1989, **37**, 2549
34 Meier, D. J. (Ed.) 'Molecular Basis for Transitions and Relaxations', Midland Macromolcular Institute Monographs, No. 4, 1978
35 Booij, H. C. and Palmen, J. H. M. *Rheol. Acta* 1982, **21**, 376
36 Scholtens, B. J. R. and Booij, H. G. in 'Elastomers and Rubber Elasticity' (Eds J. E. Marks and J. Hal), *Am. Chem. Soc. Symp. Ser.* 1982, **139**, 517